

Motion-light parametric amplifier and entanglement distributor

A. Peng and A. S. Parkins*

Department of Physics, University of Auckland, Private Bag 92019, Auckland, New Zealand.

(Dated: November 21, 2018)

We propose a scheme for entangling the motional mode of a trapped atom with a propagating light field via a cavity-mediated parametric interaction. We then show that if this light field is subsequently coupled to a second distant atom via a cavity-mediated linear-mixing interaction, it is possible to transfer the entanglement from the light beam to the motional mode of the second atom to create an EPR-type entangled state of the positions and momenta of two distantly-separated atoms.

PACS numbers: 03.67.Hk, 32.80.Lg, 42.50.-p

I. INTRODUCTION

The generation, distribution, and application of continuous variable quantum entanglement are topics of considerable interest at present, spurred on in large part by the burgeoning fields of quantum communication and quantum computation. In this context, a variety of protocols for continuous quantum variables have been proposed and in some cases already demonstrated, including quantum teleportation [1, 2, 3], quantum cryptography [4, 5, 6, 7], quantum dense coding [8, 9, 10], and quantum computation [11].

These protocols have in large part focussed on implementations involving nonlinear optics and propagating light fields, which has obvious advantages in terms of long-distance communication and existing quantum-optical technology. However, for purposes of storage (i.e., memory) and local manipulation, a number of alternative physical systems are being actively investigated and appear very promising; notably, collective atomic spin systems [12, 13, 14, 15, 16, 17, 18] and quantized vibrational states of trapped atoms [19, 20, 21, 22, 23]. Of particular interest is the capability of establishing long-lived entanglement of the Einstein-Podolsky-Rosen (EPR) type [24] between actual or effective position and momentum variables of two separated atomic systems. This capability has in fact been demonstrated recently in an experiment involving collective spins of a pair of atomic ensembles and nonlocal Bell measurements using off-resonant light pulses [18].

A scheme for preparing an EPR-type state of the actual positions and momenta of a pair of atoms has been put forward in [20], making use of interactions in cavity quantum electrodynamics (cavity QED) to facilitate the transfer of quantum correlations from light fields to motional modes of tightly trapped atoms. The source of the quantum-correlated light fields was taken to be an optical nondegenerate parametric amplifier (see, e.g., [25, 26]).

Here, we present an alternative approach to preparing such a motional state which, in contrast to the scheme

of [20], does not require a separate source of quantum-correlated light beams. Furthermore, unlike a number of other proposals, it does not require entangling measurements to be made, or a carefully timed sequence of suitably shaped light pulses. Through an atom-cavity coupling similar to, but modified from that of [20], an effective parametric interaction between cavity and motional modes generates continuous variable entanglement between the motion of the trapped atom and the light field exiting the cavity. The entanglement “carried” by this light field can subsequently be distributed to a distant location and thence to another atom (or atoms).

II. THE MODEL

The essential details of the scheme to be described in this work are illustrated in Fig. 1. A pair of atoms are harmonically confined inside separate optical cavities, with the light exiting one of the cavities coupled into the second cavity (but not vice-versa). Auxiliary lasers, incident through the sides of the cavities, combine with the cavity fields to drive Raman transitions between neighbouring vibrational levels of the motion of each atom. Note that only a single internal atomic state (i.e., a stable ground electronic state) is assumed to be involved, as will be discussed below.

A. Motion-Light Coupling

The laser-atom-cavity interactions responsible for the coupling between motional and light modes have been discussed in detail previously (see, e.g., [19, 22]), but for completeness we include a brief description. Considering just a single-atom configuration, our system is modeled, in a frame rotating at the laser frequency ω_L , by the Hamiltonian

$$\begin{aligned} H_0 = & \sum_{j=x,y,z} \hbar\nu_j (b_j^\dagger b_j + \frac{1}{2}) \\ & + \hbar\delta a^\dagger a + \hbar\Delta\sigma_+\sigma_- \\ & + \hbar[\mathcal{E}_L(y, z, t)\sigma_+ + \mathcal{E}_L^*(y, z, t)\sigma_-] \end{aligned}$$

*Corresponding author. Email address: s.parkins@auckland.ac.nz

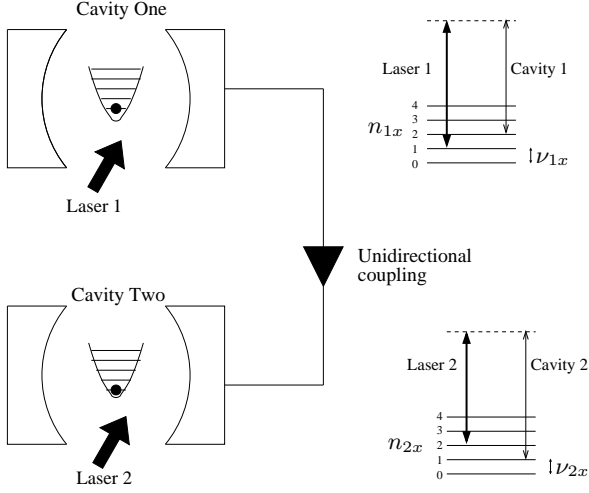


FIG. 1: Schematic diagram of the system. Atoms inside the cavities are tightly confined in harmonic traps. The cavity and laser frequencies are chosen to drive Raman transitions between neighbouring vibrational levels of the motion.

$$+ \hbar g_0 \sin(kx)(a^\dagger \sigma_- + a \sigma_+). \quad (1)$$

The first line describes the quantized harmonic motion of the trapped atom, with b_j the annihilation operator and ν_j the vibrational frequency for motion along the j -axis. The quantized cavity mode, with annihilation operator a and frequency ω_{cav} , is detuned from the laser frequency by $\delta = \omega_{\text{cav}} - \omega_L$. The ground and excited electronic states of the atom that are coupled by the light fields, $|g\rangle$ and $|e\rangle$, are separated in energy by $\hbar\omega_0$, and the detuning of the atomic transition from the laser frequency is given by $\Delta = \omega_0 - \omega_L$; $\sigma_+ = |e\rangle\langle g|$ and $\sigma_- = |g\rangle\langle e|$ are the atomic raising and lowering operators, respectively.

The laser field is treated as a classical field of (complex) amplitude $\mathcal{E}_L(y, z, t)$ and is assumed to propagate in the yz -plane. The cavity mode is aligned along the x -axis and its coupling to the atomic transition is described by the last line in (1), where g_0 is the single-photon coupling strength and k is the wavenumber of the cavity field. The choice of a sine function, with $x = (\hbar/2m\nu_x)^{1/2}(b_x + b_x^\dagger)$ the position operator of the atom, denotes that the trap is assumed to be centered at a *node* of the cavity standing-wave field.

By taking the laser-atom detuning Δ to be large (i.e., $\Delta \gg \{\nu_x, \delta, |\mathcal{E}_L|, g_0, \gamma\}$, where γ is the spontaneous emission linewidth of the state $|e\rangle$), population of the excited internal state $|e\rangle$, and hence spontaneous emission, can be made negligible. From the Heisenberg equation of motion for the atomic lowering operator,

$$\dot{\sigma}_- = -i\Delta\sigma_- + i\mathcal{E}_L(y, z, t)\sigma_z + ig_0 \sin(kx)a\sigma_z, \quad (2)$$

one can then take

$$\sigma_- \simeq \frac{-\mathcal{E}_L(y, z, t)}{\Delta} - \frac{g_0 \sin(kx)a}{\Delta}, \quad (3)$$

noting that $\dot{\sigma}_z \simeq 0$ and $\sigma_z|g\rangle = -|g\rangle$ (i.e., setting $\sigma_z \simeq -1$ in the equation of motion for σ_-).

Now, if the size of the harmonic trap is small compared to the optical wavelength (Lamb-Dicke regime), then we can make the approximation

$$\sin(kx) \simeq \eta_x(b_x + b_x^\dagger), \quad (4)$$

where $\eta_x \ll 1$ is the Lamb-Dicke parameter. In this case, one can also assume a configuration such that the position dependence of the laser amplitude over the extent of the trap can be ignored, i.e.,

$$\mathcal{E}_L(y, z, t) \simeq \mathcal{E}_L(t)e^{-i\phi_L}, \quad \mathcal{E}_L(t) \in \mathfrak{R}, \quad (5)$$

and hence only motion along the x -axis is of relevance.

Finally, for the regimes we are most interested in, the cavity mode is only ever weakly excited. This fact, combined with the smallness of the Lamb-Dicke parameter, enables us to neglect the second term in (3) in comparison to the first term, reducing our approximate solution for σ_- to the simple form

$$\sigma_- \simeq -\frac{\mathcal{E}_L(t)e^{-i\phi_L}}{\Delta}. \quad (6)$$

Using this form, and shifting the zero of energy to remove scalar terms, the Hamiltonian describing the cavity mode and motion along the x -axis reduces to [27]

$$H_0 \simeq \hbar\nu_x b_x^\dagger b_x + \hbar\delta a^\dagger a - \frac{\hbar\eta_x g_0 \mathcal{E}_L(t)}{\Delta} (b_x + b_x^\dagger)(a^\dagger e^{-i\phi_L} + a e^{i\phi_L}). \quad (7)$$

Under suitable conditions and with appropriate choices of the cavity-laser detuning, $\delta = \omega_{\text{cav}} - \omega_L$, we are able to choose between a parametric or linear mixing interaction between the cavity and motional modes, as we now show.

B. Cavity 1: Parametric Amplification

For convenience, we now drop the subscripts x and L and use the subscript 1(2) to denote system 1(2). For cavity 1 we choose $\delta_1 = -\nu_1$. Moving to an interaction picture to remove the systematic motion associated with the first two terms of (7), we obtain

$$H_1 = \Omega_1(t) \left(a_1 b_1 e^{i\phi_1} + a_1^\dagger b_1^\dagger e^{-i\phi_1} + a_1^\dagger b_1 e^{-2i\nu_1 t - i\phi_1} + a_1 b_1^\dagger e^{2i\nu_1 t + i\phi_1} \right), \quad (8)$$

where

$$\Omega_1(t) = -\frac{\hbar\eta_1 g_1 \mathcal{E}_1(t)}{\Delta_1}. \quad (9)$$

If we now assume that the trap frequency ν_1 is large, such that $\nu_1 \gg |\Omega_1(t)|$, and also $\nu_1 \gg \kappa_1$, where κ_1 is the amplitude decay rate of the cavity field, then the rapidly

oscillating terms in (8) can be neglected in a rotating-wave approximation to give

$$H_1 = \Omega_1(t) \left(a_1^\dagger b_1 e^{i\phi_1} + a_1^\dagger b_1^\dagger e^{-i\phi_1} \right). \quad (10)$$

This is the Hamiltonian for a nondegenerate parametric amplification process and via this process continuous variable entanglement can be generated between the motional and cavity modes in system 1.

C. Cavity 2: Linear Mixing

For cavity 2 we choose $\delta_2 = \nu_2$. Moving to the appropriate interaction picture and employing the rotating-wave approximation once again under the condition that $\nu_2 \gg |\Omega_2(t)|$ and $\nu_2 \gg \kappa_2$, we derive for system 2 the effective Hamiltonian

$$H_2 = \Omega_2(t) \left(a_2^\dagger b_2 e^{-i\phi_2} + b_2^\dagger a_2 e^{i\phi_2} \right), \quad (11)$$

where

$$\Omega_2(t) = -\frac{\hbar\eta_2 g_2 \mathcal{E}_2(t)}{\Delta_2}. \quad (12)$$

This describes a linear mixing interaction which, as we shall see, can lead to an exchange of properties between the cavity and motional modes.

D. Cascaded System

Having specified the effective interactions occurring in each atom-cavity system, it should now be quite clear what our aim is. Via the parametric interaction, light in cavity mode 1 is entangled with motional mode 1. This light ultimately exits cavity 1 due to cavity decay at the rate κ_1 and it may then be coupled into cavity 2, where, through the linear mixing process, entanglement of the light field with motional mode 1 may be transferred to motional mode 2, thereby entangling the two motional modes.

To examine this transfer process in detail, we turn naturally to a cascaded systems model [28, 29, 30, 31, 32], which enables us to describe a unidirectional driving of cavity 2 with the output light from cavity 1. If we assume that the dominant input and output channel to and from each cavity is through just one of the two mirrors forming each cavity (as depicted in Fig. 1), then the master equation for our cascaded system is

$$\begin{aligned} \dot{\rho} = & -\frac{i}{\hbar}[H, \rho] \\ & + \kappa_1(2a_1\rho a_1^\dagger - a_1^\dagger a_1\rho - \rho a_1^\dagger a_1) \\ & + \kappa_2(2a_2\rho a_2^\dagger - a_2^\dagger a_2\rho - \rho a_2^\dagger a_2) \\ & - 2\sqrt{\epsilon\kappa_1\kappa_2}([a_2^\dagger, a_1\rho] + [\rho a_1^\dagger, a_2]), \end{aligned} \quad (13)$$

where

$$H = H_1 + H_2, \quad (14)$$

and the parameter ϵ , satisfying $0 \leq \epsilon \leq 1$, accounts for losses in transmission and for coupling inefficiency. Ideal transmission and coupling corresponds to $\epsilon = 1$. Note that implicit in the form (13) is the assumption that the two cavity frequencies are equal, and hence that the difference in laser frequencies is set to

$$\omega_{L1} - \omega_{L2} = \nu_1 + \nu_2. \quad (15)$$

III. ADIABATIC APPROXIMATION

In the (overdamped) regime where both κ_1 and κ_2 are much larger than the coupling rates Ω_1 and Ω_2 , our model can be simplified further by adiabatically eliminating the cavity modes from the dynamics. In particular, the master equation (4) can be written in the form

$$\dot{\rho} = (\mathcal{L}_0 + \mathcal{L}_c)\rho, \quad (16)$$

where

$$\begin{aligned} \mathcal{L}_0\rho &= -\frac{i}{\hbar}[H, \rho], \\ \mathcal{L}_c\rho &= \kappa_1(2a_1\rho a_1^\dagger - a_1^\dagger a_1\rho - \rho a_1^\dagger a_1) \\ &+ \kappa_2(2a_2\rho a_2^\dagger - a_2^\dagger a_2\rho - \rho a_2^\dagger a_2) \\ &- 2\sqrt{\epsilon\kappa_1\kappa_2}([a_2^\dagger, a_1\rho] + [\rho a_1^\dagger, a_2]). \end{aligned} \quad (18)$$

In the adiabatic limit, a master equation for the reduced density operator, ρ_b , of the motional modes alone can be derived as (see, e.g., [32])

$$\dot{\rho}_b = \text{Tr}_c \left\{ \mathcal{L}_0 \int_0^\infty d\tau e^{-\mathcal{L}_c\tau} \mathcal{L}_0 \rho_c^s \right\} \rho_b, \quad (19)$$

where the trace is taken over the cavity modes and ρ_c^s is the steady state density operator of the cavity modes satisfying $\mathcal{L}_c\rho_c^s = 0$.

Evaluation of (19) requires calculation of steady-state two-time correlation functions of the cavity operators. From the master equation $\dot{\rho}_c = \mathcal{L}_c\rho_c$ one obtains the following solutions for the mean cavity amplitudes (for $t \geq 0$)

$$\begin{aligned} \langle a_1(t) \rangle_c &= e^{-\kappa_1 t} \langle a_1(0) \rangle_c, \\ \langle a_2(t) \rangle_c &= e^{-\kappa_1 t} \langle a_2(0) \rangle_c \\ &+ \frac{2\sqrt{\kappa_1\kappa_2}\epsilon}{\kappa_2 - \kappa_1} (e^{-\kappa_2 t} - e^{-\kappa_1 t}) \langle a_1(0) \rangle_c. \end{aligned} \quad (20)$$

With $\langle a_1 a_1^\dagger \rangle_c^s = \langle a_2 a_2^\dagger \rangle_c^s = 1$ being the only nonzero steady-state equal-time correlations, the quantum regression theorem gives

$$\langle a_1(\tau) a_1^\dagger(0) \rangle_c^s = \langle a_1(0) a_1^\dagger(\tau) \rangle_c^s = e^{-\kappa_1 \tau}, \quad (22)$$

$$\langle a_2(\tau) a_2^\dagger(0) \rangle_c^s = \langle a_2(0) a_2^\dagger(\tau) \rangle_c^s = e^{-\kappa_2 \tau}, \quad (23)$$

$$\begin{aligned} \langle a_2(\tau) a_1^\dagger(0) \rangle_c^s &= \langle a_1(0) a_2^\dagger(\tau) \rangle_c^s \\ &= \frac{2\sqrt{\kappa_1\kappa_2}\epsilon}{\kappa_2 - \kappa_1} (e^{-\kappa_2 \tau} - e^{-\kappa_1 \tau}), \end{aligned} \quad (24)$$

as the only non-zero two-time correlation functions (resulting from the master equation $\dot{\rho}_c = \mathcal{L}_c \rho_c$).

Using these correlation functions in (19), the master equation for the reduced density operator of the *motional modes* is

$$\begin{aligned} \dot{\rho}_b = & \Gamma_1(2b_1^\dagger \rho_b b_1 - b_1 b_1^\dagger \rho_b - \rho_b b_1 b_1^\dagger) \\ & + \Gamma_2(2b_2 \rho_b b_2^\dagger - b_2^\dagger b_2 \rho_b - \rho_b b_2^\dagger b_2) \\ & + 2\sqrt{\epsilon \Gamma_1 \Gamma_2} \left([b_2^\dagger, b_1^\dagger \rho_b] e^{-i(\phi_1 - \phi_2)} \right. \\ & \left. + [\rho_b b_1, b_2] e^{i(\phi_1 - \phi_2)} \right), \end{aligned} \quad (25)$$

where

$$\Gamma_1 = \frac{\Omega_1^2}{\kappa_1} \quad \text{and} \quad \Gamma_2 = \frac{\Omega_2^2}{\kappa_2} \quad (26)$$

are the effective growth and decay rates, respectively, for motional modes 1 and 2. In this reduced model a direct coupling between these modes now appears in the form of the last term in (25).

IV. MOTIONAL STATE ENTANGLEMENT

A. Motional Mode Correlations

From the master equation (25), a closed set of (inhomogeneous) differential equations can be obtained for the correlation functions $\langle b_1^\dagger b_1 \rangle$, $\langle b_2^\dagger b_2 \rangle$ and $\langle b_1 b_2 \rangle$. These are (setting $\phi_1 = \phi_2$ for simplicity)

$$\begin{aligned} \dot{\langle b_1 b_2 \rangle} = & (\Gamma_1 - \Gamma_2) \langle b_1 b_2 \rangle \\ & + 2\sqrt{\epsilon \Gamma_1 \Gamma_2} (\langle b_1^\dagger b_1 \rangle + 1), \end{aligned} \quad (27)$$

$$\dot{\langle b_1^\dagger b_1 \rangle} = 2\Gamma_1(1 + \langle b_1^\dagger b_1 \rangle), \quad (28)$$

$$\begin{aligned} \dot{\langle b_2^\dagger b_2 \rangle} = & -2\Gamma_2 \langle b_2^\dagger b_2 \rangle \\ & + 2\sqrt{\epsilon \Gamma_1 \Gamma_2} (\langle b_1^\dagger b_2^\dagger \rangle + \langle b_1 b_2 \rangle), \end{aligned} \quad (29)$$

with solutions

$$\langle b_1^\dagger(t) b_1(t) \rangle = e^{2\Gamma_1 t} - 1, \quad (30)$$

$$\langle b_1(t) b_2(t) \rangle = \frac{2\sqrt{\epsilon \Gamma_1 \Gamma_2}}{\Gamma_1 + \Gamma_2} e^{\Gamma_1 t} (e^{\Gamma_1 t} - e^{-\Gamma_2 t}), \quad (31)$$

$$\langle b_2^\dagger(t) b_2(t) \rangle = \frac{4\epsilon \Gamma_1 \Gamma_2}{(\Gamma_1 + \Gamma_2)^2} (e^{\Gamma_1 t} - e^{-\Gamma_2 t})^2, \quad (32)$$

where both oscillators are assumed to have initially been in their ground states. Note that, under these conditions, $\langle b_1(t) b_1(t) \rangle = \langle b_2(t) b_2(t) \rangle = \langle b_1^\dagger(t) b_2(t) \rangle = 0$ for all t .

The growing value of $\langle b_1(t) b_2(t) \rangle$ demonstrates that our cascaded system enables correlations to develop between the two motional modes. The nature of the correlations is, not surprisingly, reminiscent of a two-mode

squeezed state and leads us to examine correlations between the positions and momenta of the trapped atoms.

Before proceeding, however, we note that the exponential growth exhibited by the mean excitation numbers must eventually become problematical for our model, since the Lamb-Dicke assumption breaks down once the excitation numbers become large enough that the physical extent of the atomic wavepacket is no longer much smaller than the wavelength of the light. We shall return to this point when we consider practical aspects of the scheme.

B. Position and Momentum Variances

Defining position and momentum operators for the motional modes as

$$X_j = b_j + b_j^\dagger, \quad P_j = -i(b_j - b_j^\dagger), \quad (j = 1, 2), \quad (33)$$

variances in the sum and difference operators are calculated to be

$$\begin{aligned} \langle (X_1 \pm X_2)^2 \rangle &= \langle (P_1 \mp P_2)^2 \rangle \\ &= 2 \left[e^{\Gamma_1 t} \pm \frac{2\sqrt{\epsilon \Gamma_1 \Gamma_2}}{\Gamma_1 + \Gamma_2} (e^{\Gamma_1 t} - e^{-\Gamma_2 t}) \right]^2, \end{aligned} \quad (34)$$

where the ‘‘vacuum’’ level (i.e., where the atoms are both in their ground motional states) is 2. We note first that, since $(e^{\Gamma_1 t} - e^{-\Gamma_2 t}) \geq 0$, $\langle (X_1 + X_2)^2 \rangle = \langle (P_1 - P_2)^2 \rangle \geq 2$ at all times, i.e., these variances are only ever increased compared to the vacuum level.

However, the variances $\langle (X_1 - X_2)^2 \rangle$ and $\langle (P_1 + P_2)^2 \rangle$ can be reduced below the value of 2, as illustrated in Fig. 2, where $\langle (X_1 - X_2)^2 \rangle$ is plotted as a function of time for various values of the ratio Γ_2/Γ_1 , and with $\epsilon = 1$. The case $\Gamma_2/\Gamma_1 = 1$, where the effective damping rates of the two motional modes are equal, is particularly interesting and leads to the simplified result

$$\begin{aligned} \langle (X_1 - X_2)^2 \rangle &= \langle (P_1 + P_2)^2 \rangle \\ &= 2e^{-2\Gamma_1 t} \rightarrow 0 \quad \text{as } t \rightarrow \infty. \end{aligned} \quad (35)$$

So, using this scheme it is, in principle, possible to produce a state corresponding to perfectly correlated positions and perfectly anti-correlated momenta of the two atoms, i.e., to produce an EPR state. Once again, in comparing this approach to that of [20], it should be emphasized that the present scheme *does not require a separate source of entangled light beams*.

If $\Gamma_2/\Gamma_1 \neq 1$ and/or $\epsilon < 1$, then the variance $\langle (X_1 - X_2)^2 \rangle$ attains a finite minimum value at a particular time, after which it increases indefinitely. Defining $\lambda = \Gamma_2/\Gamma_1$, this minimum value is calculated to be

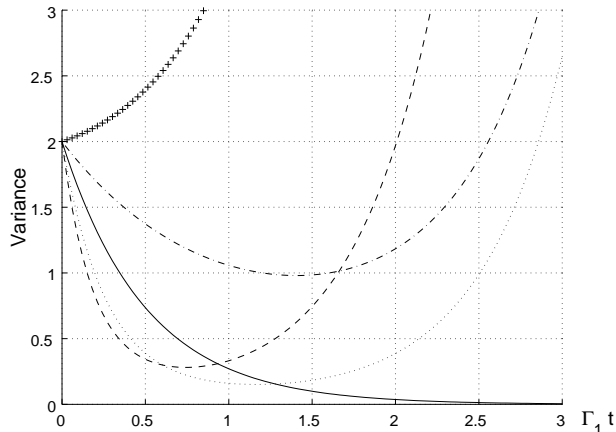


FIG. 2: The variance $\langle (X_1 - X_2)^2 \rangle$ as a function of time for $\Gamma_2/\Gamma_1 = 0.2$ (pluses), $\Gamma_2/\Gamma_1 = 0.5$ (dot-dashed line), $\Gamma_2/\Gamma_1 = 1$ (solid line), $\Gamma_2/\Gamma_1 = 2$ (dotted line), and $\Gamma_2/\Gamma_1 = 3$ (dashed line). The coupling is taken to be ideal, i.e., $\epsilon = 1$.

$$\langle (X_1 - X_2)^2 \rangle_{\min} = \frac{2}{(1 + \lambda)^2} \left[\frac{(2\sqrt{\epsilon}\lambda^{\frac{3}{2}})^{\frac{1}{1+\lambda}}}{(1 + \lambda - 2\sqrt{\lambda\epsilon})^{\frac{1}{1+\lambda}-1}} + 2\sqrt{\lambda\epsilon} \left(\frac{2\sqrt{\epsilon}\lambda^{\frac{3}{2}}}{1 + \lambda - 2\sqrt{\lambda\epsilon}} \right)^{\frac{-\lambda}{1+\lambda}} \right]^2, \quad (36)$$

and the time at which the minimum value occurs is given by

$$\Gamma_1 t_{\min}(\lambda) = \frac{1}{1 + \lambda} \ln \left[\frac{2\lambda\sqrt{\lambda\epsilon}}{1 + \lambda - 2\sqrt{\lambda\epsilon}} \right]. \quad (37)$$

Plots of $\langle (X_1 - X_2)^2 \rangle_{\min}$ and $\Gamma_1 t_{\min}$ versus λ are shown in Figs. 3 and 4 for several values of ϵ . Note that $t_{\min} > 0$ only where $\lambda > 1/(4\epsilon)$. If $\lambda < 1/(4\epsilon)$ then there is no reduction in the variance below the vacuum level.

From Figs. 3 and 4 (in particular, from their asymmetry about the point $\lambda = 1$), it is clear that the scheme generally performs best in the regime where $\Gamma_2 \geq \Gamma_1$ (i.e., $\lambda \geq 1$). In particular, significant reductions in the variances below the vacuum level occur over a broad region of Γ_2 values, provided $\Gamma_2 \geq \Gamma_1$.

With decreasing values of the parameter ϵ (i.e., with decreasing coupling efficiency or increasing transmission losses), the minimum attainable variance increases and occurs for larger values of λ and at somewhat earlier times. It follows that, for a realistic system with $\epsilon < 1$, it would be advantageous to work in a regime with $\Gamma_2 > \Gamma_1$. This is further illustrated in Fig. 5, where the variance is again plotted as a function of time, but now for several combinations of λ and ϵ . It is worth noting that a significant reduction in the variance ($\sim 73\%$) is still possible with $\epsilon = 0.8$, i.e., $\langle (X_1 - X_2)^2 \rangle_{\min} \simeq 0.54$ at $\Gamma_1 t_{\min} \simeq 0.8$ for $\lambda = 2$.

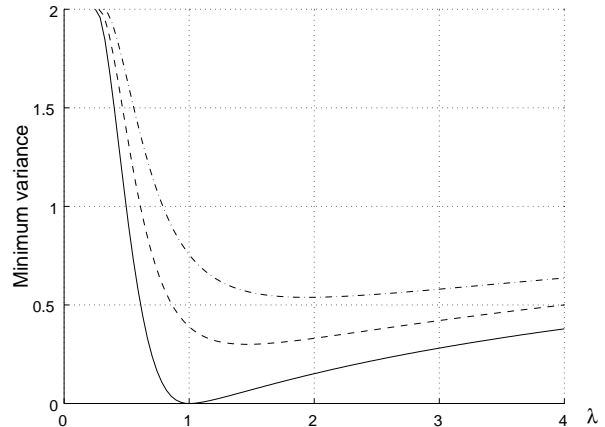


FIG. 3: Minimum variance $\langle (X_1 - X_2)^2 \rangle_{\min}$ as a function of $\lambda = \Gamma_2/\Gamma_1$ for $\epsilon = 1$ (solid line), $\epsilon = 0.9$ (dashed line) (minimum value of 0.30 at $\lambda = 1.46$), and $\epsilon = 0.8$ (dot-dashed line) (minimum value of 0.54 at $\lambda = 1.95$).

It should also be noted that, for the examples chosen in the regime where $\epsilon < 1$ and $\lambda \geq 1$, the minimum variance generally occurs at times $\Gamma_1 t$ of the order of 1. The mean excitation number for motional mode 1, $\langle b_1^\dagger b_1 \rangle$, is then of the order of $e^2 - 1 \simeq 6$, with a slightly smaller value for $\langle b_2^\dagger b_2 \rangle$.

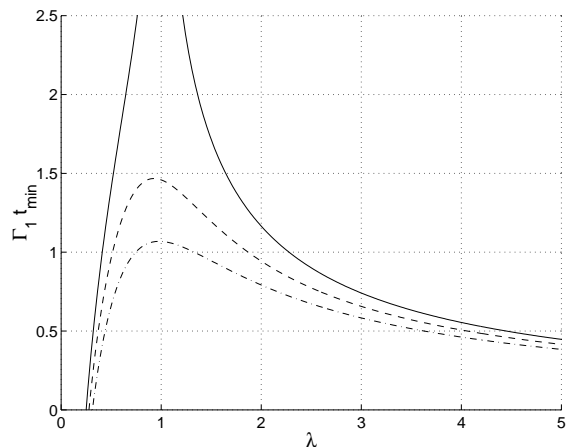


FIG. 4: Time at which minimum variance occurs, $\Gamma_1 t_{\min}$, as a function of $\lambda = \Gamma_2/\Gamma_1$ for $\epsilon = 1$ (solid line), $\epsilon = 0.9$ (dashed line), and $\epsilon = 0.8$ (dot-dashed line).

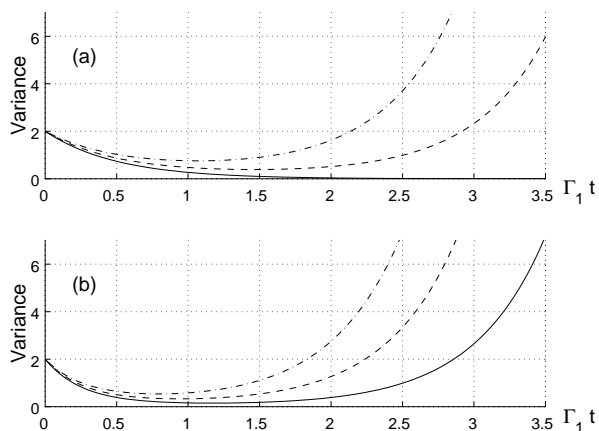


FIG. 5: Variance $\langle (X_1 - X_2)^2 \rangle$ as a function of time for (a) $\lambda = 1$ and (b) $\lambda = 2$, with $\epsilon = 1$ (solid line), $\epsilon = 0.9$ (dashed line), and $\epsilon = 0.8$ (dot-dashed line).

V. COMPARISON WITH NUMERICAL CALCULATIONS

Starting from the master equation (13), which includes the cavity dynamics, a closed set of differential equations can be obtained for various correlation functions of the system. We have integrated these equations numerically (using a 4th-order Runge-Kutta method) and computed the variance $\langle (X_1 - X_2)^2 \rangle$ for comparison with the results of the adiabatic approximation. This comparison is presented in Figs. 6 and 7 for several example sets of parameters.

On the timescales shown, the adiabatic approximation is seen to work well provided the coupling strengths Ω_j are, roughly, at least five to ten times smaller than the cavity decay rates κ_j . For larger values of Ω_j the maximum degree of reduction in the variance is significantly

reduced and the dynamics obviously become somewhat more complicated, e.g., oscillatory behaviour starts to feature and excitation of the cavity modes increases.

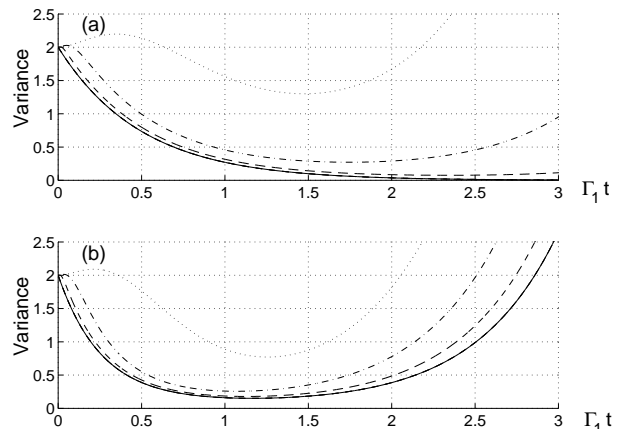


FIG. 6: Comparison of numerical and adiabatic approximation results for $\langle (X_1 - X_2)^2 \rangle$ versus time with $\kappa_1 = \kappa_2 = 1$. The adiabatic approximation is shown in each plot as a solid line. (a) $\lambda = 1$, with $\Omega_1 = \Omega_2 = 0.1$ (dashed line), $\Omega_1 = \Omega_2 = 0.2$ (dot-dashed line), $\Omega_1 = \Omega_2 = 0.5$ (dotted line). (b) $\lambda = 2$, with $\Omega_1 = 0.1$, $\Omega_2 = \sqrt{2} \times 0.1$ (dashed line), $\Omega_1 = 0.2$, $\Omega_2 = \sqrt{2} \times 0.2$ (dot-dashed line), $\Omega_1 = 0.5$, $\Omega_2 = \sqrt{2} \times 0.5$ (dotted line).

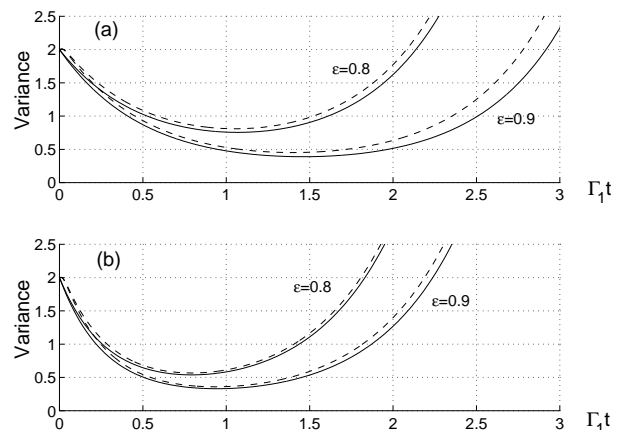


FIG. 7: Comparison of numerical and adiabatic approximation results for $\langle (X_1 - X_2)^2 \rangle$ versus time with $\kappa_1 = \kappa_2 = 1$ and nonideal coupling between the cavities (i.e., $\epsilon < 1$). The adiabatic approximation is shown in each plot as a solid line. (a) $\lambda = 1$, with $\Omega_1 = \Omega_2 = 0.1$ (dashed lines). (b) $\lambda = 2$, with $\Omega_1 = 0.1$, $\Omega_2 = \sqrt{2} \times 0.1$ (dashed lines).

VI. PRACTICAL CONSIDERATIONS

We now consider in slightly more detail the conditions under which the most significant assumptions required by

our model should be satisfied. Firstly though, as a more general comment, we note that exciting progress has been made recently in experimental cavity QED with single trapped atoms or ions [33, 34, 35, 36, 37]. In fact, various “ingredients” of the scheme presented in this work have already been demonstrated.

A. Trap Frequency

The neglect of terms in the effective motion-cavity mode interaction Hamiltonians which vary like $e^{\pm 2i\nu_j t}$ requires that the trap frequencies be large in comparison with the cavity decay rates κ_j and the effective coupling parameters Ω_j . To quantify this a little more precisely, previous numerical studies have shown that this rotating-wave approximation is very good provided the trap frequencies are at least an order of magnitude larger than κ_j and Ω_j [19, 22]. We note that an experimental situation with $\nu_j \gg \kappa$ has been realized recently with single calcium ions trapped inside a high-finesse optical cavity [37].

B. Lamb-Dicke Approximation

The Lamb-Dicke approximation has been examined in some detail in [22]. Taking into account the spread of the phonon number distribution associated with a general state, a condition for the validity of this approximation can be derived as

$$\frac{1}{2}\eta_x^2(1 + \bar{n}_x + a\sigma_{\bar{n}_x}) \ll 1, \quad (38)$$

where \bar{n}_x is the mean phonon number, $\sigma_{\bar{n}_x}^2$ is the variance of the number state distribution, and $a \sim 2 - 3$ (i.e., a few standard deviations from the mean). If we assume that the number state distribution of each mode is close to that of a thermal mode, then we can take $\sigma_{\bar{n}_x} \simeq (\bar{n}_x^2 + \bar{n}_x)^{1/2} \simeq \bar{n}_x + 1/2$ for $\bar{n}_x > 2$, and, with $a = 3$, the condition becomes

$$\bar{n}_x \ll \frac{1}{2\eta_x^2} - \frac{5}{8}. \quad (39)$$

For $\eta_x = 0.1$ this reduces to $\bar{n}_x \ll 49$. As noted earlier, at the time when minimum variances are generally achieved by our scheme (e.g., with $\epsilon < 1$ and $\lambda \geq 1$), the mean phonon excitation numbers are of the order of 5–6, suggesting that Lamb-Dicke parameters of the order of 0.1 or smaller are sufficient.

Such values of the Lamb-Dicke parameter have been achieved with single atoms in cavity QED settings [33, 36, 37]. An ability to position the trap center very precisely at any point along the cavity standing wave field (e.g., at a node of the field, as required by the present scheme) has also been demonstrated [36, 37].

Before continuing, we briefly mention the further interesting possibility of introducing a nontrivial time dependence to one or both of the coupling laser fields. One such example is illustrated in Fig. 8. Here, $\Omega_2 = 1$ (in dimensionless units) is fixed, while $\Omega_1(t) = \Omega_2 \sin(t/\tau)$ ($\tau = 20, 25, 30$), i.e., the effective parametric coupling strength is slowly increased from zero in the first atom-cavity system. If we consider the point for each case at which the variance is reduced to 0.2 (i.e., a 90% reduction below the “vacuum” level), then the corresponding mean phonon number at this time is seen to be only of the order of 2–3 for time-dependent $\Omega_1(t)$, whereas for the case of constant Ω_1 and Ω_2 (also shown in the figures) a variance of 0.2 is only attained with a mean phonon number greater than 10.

We have not explored other time dependencies in detail, but it would appear that there could be some advantage to doing so, in particular, from the point of view of minimizing the variance while maintaining mean phonon excitation numbers which comfortably satisfy the Lamb-Dicke constraint.

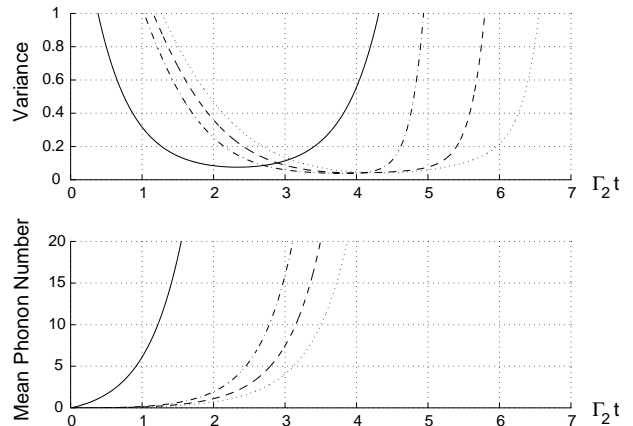


FIG. 8: Variance $\langle (X_1 - X_2)^2 \rangle$ and mean phonon number $\langle b_1^\dagger b_1 \rangle$ as a function of time from numerical simulation of Eq. (13) using $\epsilon = 1$, $\kappa_1 = \kappa_2 = 10$, $\Omega_2 = 1$ ($\Gamma_2 = \Omega_2^2/\kappa_2 = 0.1$), and $\Omega_1(t) = \Omega_2 \sin(t/20)$ (dot-dashed line), $\Omega_1(t) = \Omega_2 \sin(t/25)$ (dashed line), $\Omega_1(t) = \Omega_2 \sin(t/30)$ (dotted line). The case $\Omega_1 = \Omega_2 = 1$ is shown as a solid line.

C. Atomic Spontaneous Emission

In practice, finite excitation of the atomic excited state will introduce the effects of spontaneous emission to the dynamics. Random momentum recoils associated with spontaneous emission events will disturb the motional states in an uncontrollable manner. However, if the rate at which such events occur is small compared with the rate at which the entangled states of interest are prepared by our scheme, then the effects of spontaneous emission can essentially be neglected.

In [22] the rate of spontaneous emission events affecting the motional state is estimated for the kind of configuration we are considering here. By comparing this rate with the rates Γ_i , which characterize the preparation of the entangled motional states, the general condition under which the effects of spontaneous emission can be neglected is derived to be

$$\frac{10g_0^2}{\kappa\gamma} \gg 1, \quad (40)$$

where γ is the linewidth (FWHM) of the internal atomic excited state. This is basically the condition of strong-coupling cavity QED, as realized, for example, in the single-atom experiments of [33, 34, 35] (where values of $g_0^2/(\kappa\gamma)$ in the range 30–150 were achieved).

Finally, note that throughout this work we have neglected any forms of motional state decoherence associated with the trap itself. This seems reasonable, at least in the case of trapped ions, where typical timescales for motional decoherence and heating observed in recent experiments are of the order of milliseconds or longer [38, 39]. With values of g_0 and κ in the MHz range, we would anticipate a timescale for preparation of the motional states (i.e., Γ_i^{-1}) that is more than an order of magnitude shorter than such decoherence times.

VII. CONCLUSIONS

In conclusion, we have described a scheme for entangling motional and light-field modes via an effective para-

metric (or two-mode squeezing) interaction realized in a single-atom cavity QED setting. Through decay of the cavity field through one of its mirrors, the cavity field entanglement is transferred to an external propagating field which may be coupled to the motional mode of a distant atom via a second cavity-QED-mediated interaction. This enables the preparation of an EPR-type entangled state of the position and momentum variables of separated atoms. This has a distinct advantage over a related scheme [20] for preparing such a state in that a separate source of entangled light beams is *not* required.

We have given consideration to various practical issues associated with the scheme and pointed to a variety of recent experiments in single-atom cavity QED which collectively offer great encouragement to our proposal. Realization of the scheme would offer the exciting possibility of implementing a variety of continuous variable quantum computation and communication protocols, as well as opening the door to further investigations of fundamental aspects of entangled quantum systems, only now with distantly-separated *massive* particles [20].

Acknowledgments

AP was supported by a University of Auckland Summer Studentship. ASP acknowledges support from the Marsden Fund of the Royal Society of New Zealand and thanks Lu-Ming Duan for discussions related to this work.

-
- [1] L. Vaidman, Phys. Rev. A **49**, 1473 (1994).
 - [2] S. L. Braunstein and H. J. Kimble, Phys. Rev. Lett. **80**, 869 (1998).
 - [3] A. Furusawa *et al.*, Science **282**, 706 (1998).
 - [4] T. C. Ralph, Phys. Rev. A **61**, 010303(R) (2000).
 - [5] M. Hillery, Phys. Rev. A **61**, 022309 (2000).
 - [6] S. F. Pereira, Z. Y. Ou, and H. J. Kimble, Phys. Rev. A **62**, 042311 (2000).
 - [7] M. D. Reid, Phys. Rev. A **62**, 062308 (2000).
 - [8] M. Ban, J. Opt. B: Quantum Semiclass. Opt. **1**, L9 (1999).
 - [9] S. L. Braunstein and H. J. Kimble, Phys. Rev. A **61**, 042302 (2000).
 - [10] X. Li *et al.*, Phys. Rev. Lett. **88**, 047904 (2002).
 - [11] S. Lloyd and S. L. Braunstein, Phys. Rev. Lett. **82**, 1784 (1999).
 - [12] M. D. Lukin, S. F. Yelin, and M. Fleischhauer, Phys. Rev. Lett. **84**, 4232 (2000).
 - [13] A. Mair *et al.*, Phys. Rev. A **65**, 031802 (2002).
 - [14] A. V. Turukhin *et al.*, Phys. Rev. Lett. **88**, 023602 (2002).
 - [15] A. S. Zibrov *et al.*, Phys. Rev. Lett. **88**, 103601 (2002).
 - [16] A. E. Kozhekin, K. Mølmer, and E. Polzik, Phys. Rev. A **62**, 033809 (2000).
 - [17] L.-M. Duan, J. I. Cirac, P. Zoller, and E. S. Polzik, Phys. Rev. Lett. **85**, 5643 (2000).
 - [18] B. Julsgaard, A. Kozhekin, and E. S. Polzik, Nature **413**, 400 (2001).
 - [19] A. S. Parkins and H. J. Kimble, J. Opt. B: Quantum Semiclass. Opt. **1**, 496 (1999).
 - [20] A. S. Parkins and H. J. Kimble, Phys. Rev. A **61**, 052104 (2000).
 - [21] A. S. Parkins and H. J. Kimble, in *Frontiers of Laser Physics and Quantum Optics, Proceedings of the International Conference on Laser Physics and Quantum Optics*, edited by Z. Xu, S. Xie, S.-Y. Zhu, and M. O. Scully (Springer, Berlin, 2000), p. 321. See also quant-ph/9909021.
 - [22] A. S. Parkins and E. Larsabal, Phys. Rev. A **63**, 012304 (2001).
 - [23] S. Mancini and S. Bose, Phys. Rev. A **64**, 032308 (2001).
 - [24] A. Einstein, B. Podolsky, and N. Rosen, Phys. Rev. **47**, 777 (1935).
 - [25] Z. Y. Ou, S. F. Pereira, H. J. Kimble, and K. C. Peng, Phys. Rev. Lett. **68**, 3663 (1992).
 - [26] Z. Y. Ou, S. F. Pereira, and H. J. Kimble, Appl. Phys. B: Photophys. Laser Chem. **55**, 265 (1992).
 - [27] H. Zeng and F. Lin, Phys. Rev. A **50**, R3589 (1994).
 - [28] C. W. Gardiner, Phys. Rev. Lett. **70**, 2269 (1993).

- [29] H. J. Carmichael, Phys. Rev. Lett. **70**, 2273 (1993).
- [30] P. Kochan and H. J. Carmichael, Phys. Rev. A **50**, 1700 (1994).
- [31] C. W. Gardiner and A. S. Parkins, Phys. Rev. A **50**, 1792 (1994).
- [32] C. W. Gardiner and P. Zoller, *Quantum Noise* (Springer, Berlin, 2000).
- [33] J. Ye, D. Vernooy, and H. J. Kimble, Phys. Rev. Lett. **83**, 4987 (1999).
- [34] C. J. Hood *et al.*, Science **287**, 1447 (2000).
- [35] P. W. H. Pinkse, T. Fischer, P. Maunz, and G. Rempe, Nature **404**, 365 (2000).
- [36] G. R. Guthöhrlein *et al.*, Nature **414**, 49 (2001).
- [37] A. B. Mundt *et al.*, preprint, quant-ph/0202112.
- [38] Ch. Roos *et al.*, Phys. Rev. Lett. **83**, 4713 (1999).
- [39] Q.A. Turchette *et al.*, Phys. Rev. A **61**, 063418 (2000).